Supplementary Information for

"Tunable hybridized plasmon-phonon in graphene/ mica-nanofilm heterostructure"

Yaling Qin[† a,b], Min Liu[†a,b], Hanchao Teng [b,c], Na Chen [b,c], Chenchen Wu [b,c], Chengyu Jiang [b,c], Zhuoxin Xue [b,c], Hualong Zhu [b,c], Jiayi Gui [b,c], Xiang Liu[d*], Yuchuan Xiao [b,c *], Hai Hu [b,c *]

a. School of Materials Science and Engineering, Henan Institute of Advanced Technology, Zhengzhou University, Zhengzhou,450001, China.
b. CAS Key Laboratory of Nanophotonic Materials and Devices, CAS Key Laboratory of Standardization and Measurement for Nanotechnology, National Center for Nanoscience and Technology, Beijing 100190, P. R. China.
c. Center of Materials Science and Optoelectronics Engineering, University of Chinese Academy of Sciences, Beijing 100049, P. R. China.
d. Nanjing University of Information Science and Technology, Nanjing, 210044 China.
† These authors contributed equally
*e-mail: huh@nanoctr.cn, xiaoyc@nanoctr.cn, 002821@nuist.edu.cn

This PDF file includes:

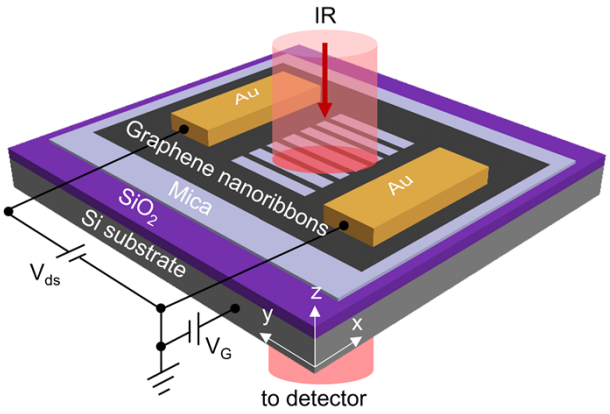

Supplementary Figure 1. Configuration of the light beam and gate circuit during infrared spectroscopy measurement.

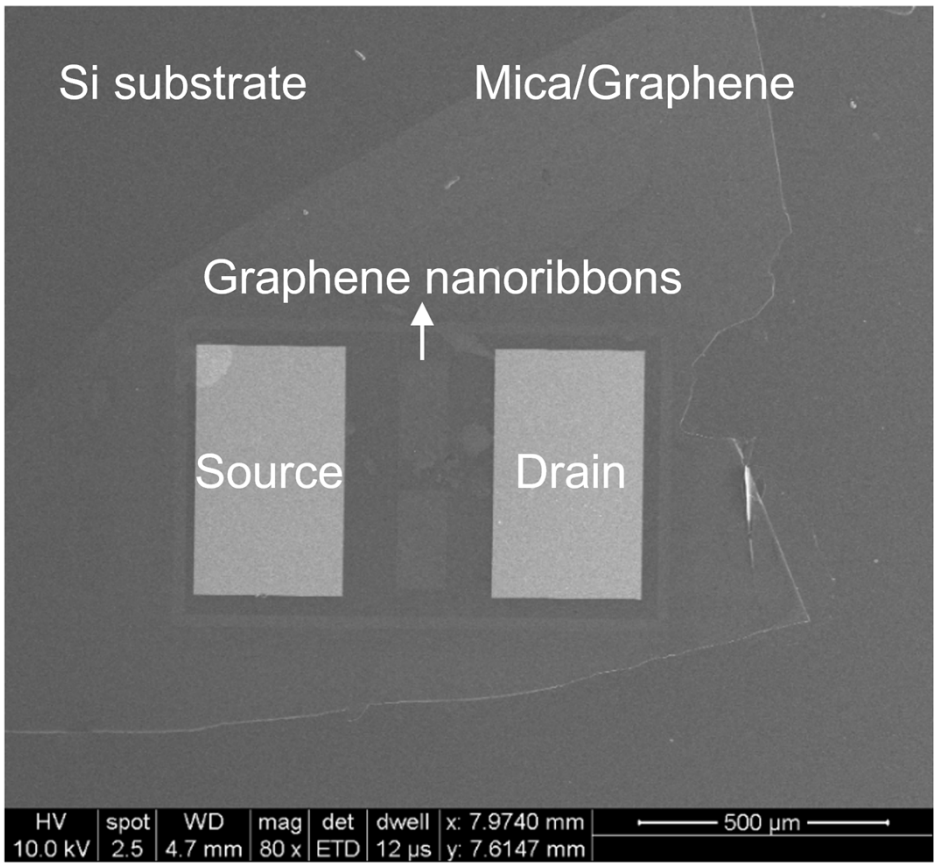

Supplementary Figure 2. Scanning electron microscope (SEM) image of the sample in Figure 1 of the main text.

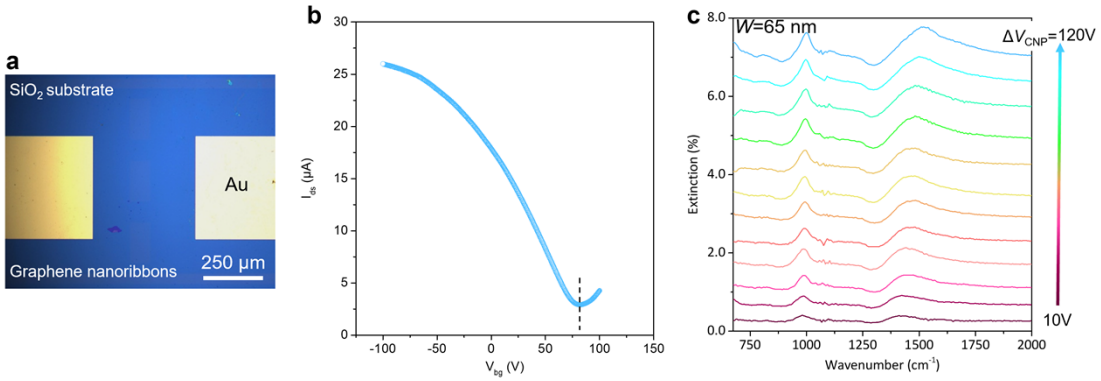

Supplementary Figure 3. Graphene plasmons on a silicon oxide substrate as a control experiment for graphene plasmons on a mica substrate. (**a**) Optical image of the sample. The scale bar indicates 250 μm. (**b**) Transfer curve of the device. (**c**) Extinction spectra of graphene nanoribbon regions on the silicon substrate under different gate voltages. The voltage difference (ΔV_{CNP}) between the applied gate voltage and the CNP increases from 10 V to 120 V.

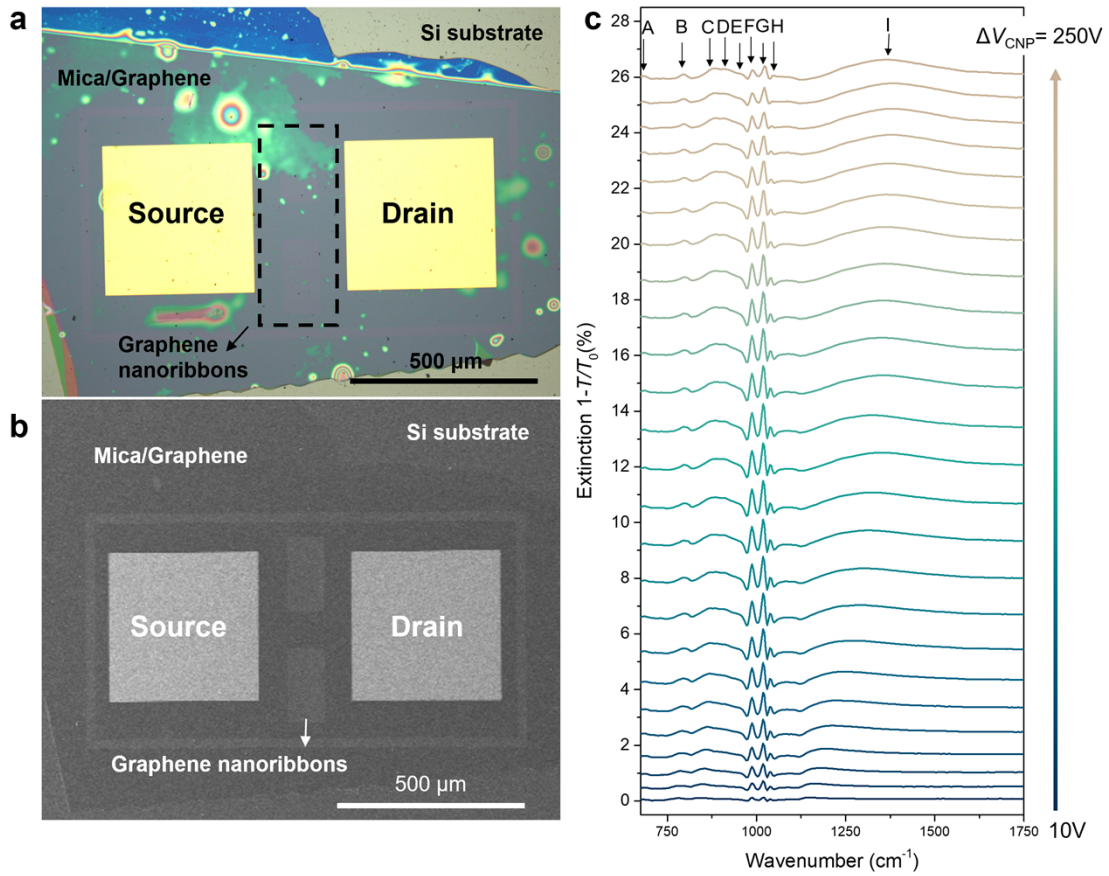

Supplementary Figure 4. Device reproducibility. (**a**) Optical image of device 2#. The highlighted area enclosed by the black dashed box denotes the region of graphene nanoribbons. The width of the fabricated ribbons is approximately 60 nm, with a gap width of around 100 nm. The scale bar indicates 500 μm. (**b**) Scanning electron microscope (SEM) image of device 2. (**c**) Extinction spectra of graphene nanoribbon regions under different gate voltages. The voltage difference (ΔV_{CNP}) between the applied gate voltage and the CNP increases from 10 V to 250 V. Peaks in the curve are labeled as alphabet A-I.

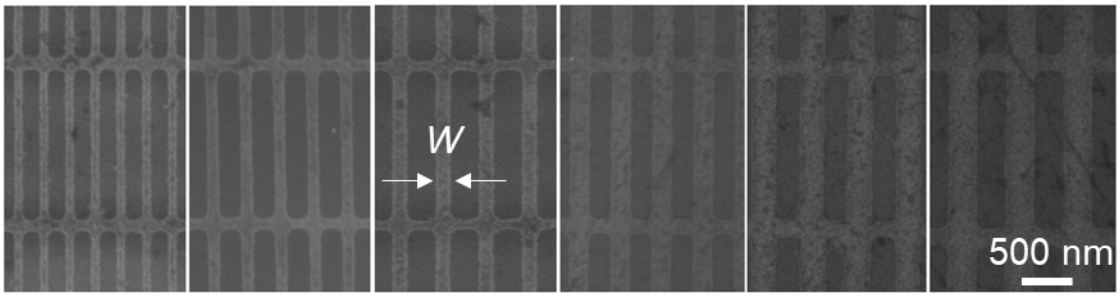

Supplementary Figure 5. SEM images of different widths of graphene nanoribbons. The scale bar indicates 500 nm.

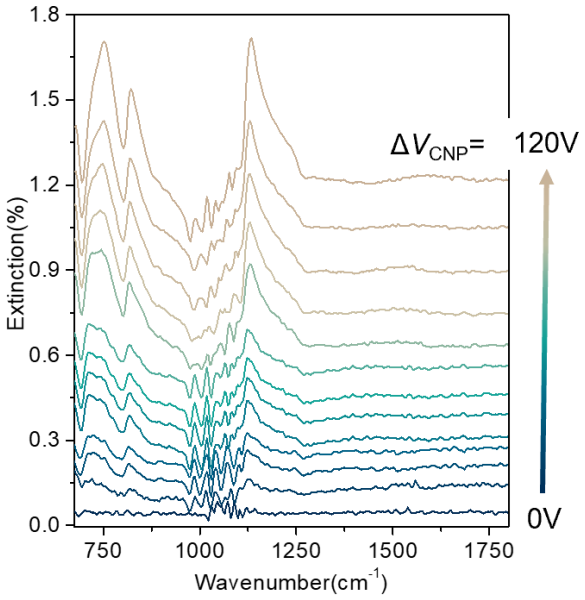

Supplementary Figure 6. Extinction spectra of graphene nanoribbon on the mica/SiO_2 substrate under different gate voltages. The voltage difference (ΔV_{CNP}) between the applied gate voltage and the CNP increases from 0 V to 120 V.

Supplementary Note 1. Spectral simulation.

To better understand the coupling between different modes, we have provided both simulation and theoretical derivation analysis. First, it is crucial to obtain reliable mica parameters before considering the coupling between graphene plasmons and mica phonons. We assume the incident light is normal to the semi-infinite mica substrate and the amplitude reflection and transmission coefficients (r_{12} and t_{12}) are depicted below:

$$r_{12} = \frac{\sqrt{\varepsilon_a} - \sqrt{\varepsilon_m}}{\sqrt{\varepsilon_a} + \sqrt{\varepsilon_m}}, \#(S1)$$

$$t_{12} = \frac{2\sqrt{\varepsilon_a}}{\sqrt{\varepsilon_m} + \sqrt{\varepsilon_a}}, \#(S2)$$

where ε_a and ε_m depict the permittivity of air and mica substrate.

Considering the thickness of mica is finite (t_m = 280 nm), as shown in Supplementary Figure 7a, we need to account for the interference phenomena between reflection and transmission to revise the effective reflection and transmission through multiple layers. The total reflection and transmission can be expressed as follows:

$$r_{total} = r_{12} + \frac{r_{23}\exp\left(2ik_z t_m\right)}{1 - r_{23}r_{21}\exp\left(2ik_z t_m\right)}, \#(S3)$$

$$t_{total} = \frac{t_{12}t_{23}\exp\left(2ik_z t_m\right)}{1 - r_{23}r_{21}\exp\left(2ik_z t_m\right)}, \#(S4)$$

where r_{12}, t_{12}, r_{23}, t_{23} denote the reflection and transmission coefficients across the interface air/mica and mica/Si, respectively, and t_m is the thickness of the mica layer. When t_m is 0 nm, implying the absence of a mica layer, the equation $S3$ and $S4$ reduces to equation $S1$ and $S2$. Taking into account the presence of a silicon substrate, the total extinction spectrum in the experiments can be expressed as:

$$I_E = 1 - \left(\frac{t_{total}(\, t_m = 280\ nm)}{t_{total}(\, t_m = 0\ nm)}\right)^2, \#(S5)$$

where $t_{total}(\, t_m = 280\ nm)$ and $t_{total}(\, t_m = 0\ nm)$ depict the transmission of the

air/mica/Si substrate and air/Si substrate, respectively.

To obtain the mica optical parameter, we use an analytical model based on the sum of Lorentz oscillators. The model is of the following form:

$$\varepsilon_m = \varepsilon_\infty + \sum_{i=1}^{n} \frac{f_i^2}{\omega_i^2 - \omega^2 - i\gamma_i\omega}, \#(S6)$$

where $\varepsilon_\infty = 1$ is a constant dielectric background and f_i, γ_i and ω_i are parameters characterizing individual vibrations of mica. Combining equations $S5$ and $S6$, we can obtain the mica optical parameter as shown in Supplementary Figure 7b.

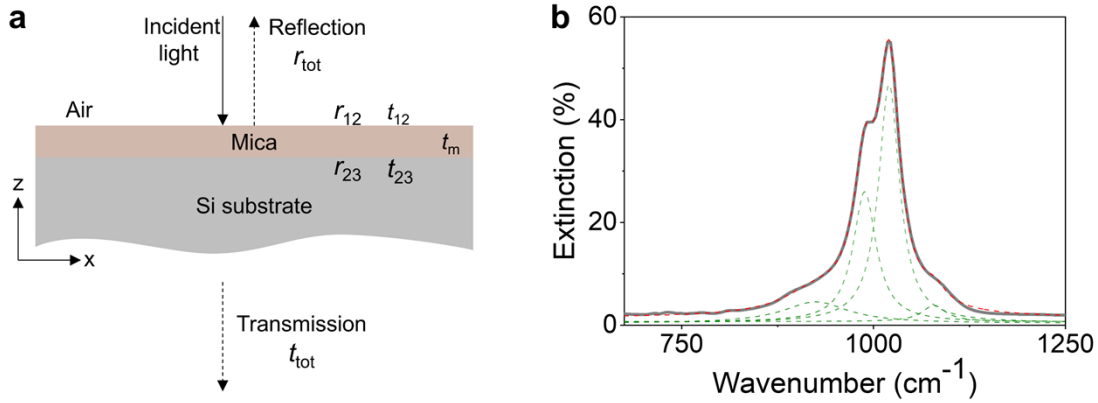

Supplementary Figure 7. Fitting extinction spectra of mica film. (a) Schematic diagram illustrating the sample structure and measurement of extinction spectra. **(b)** Extinction spectra of mica film. The gray solid line represents the experimental data. The four green dashed curves represent the fitting results through equations $S5$ and $S6$. The red dashed curve represents the cumulative data of all the green peaks.

We further investigate the coupling between graphene ribbons and mica film. Similar to the experimental setup, we have designed a four-layer structure as shown in Supplementary Figure 8a, The electrical conductivity of the graphene plasmon is adopted from the Kubo conductivity formula:

$$\sigma(\omega) = \frac{ie^2 K_B T\left(\omega + \frac{1}{\tau}\right)}{\pi\hbar^2}\left[\frac{E_F}{K_B T} + 2\ln\left(exp\left(-\frac{E_F}{K_B T}\right) + 1\right)\right] + i\frac{e^2}{4\pi\hbar} ln\left[\frac{2|E_F| - \hbar\left(\omega + \frac{i}{\tau}\right)}{2|E_F| + \hbar\left(\omega + \frac{i}{\tau}\right)}\right], \#(S7)$$

which depends on the Fermi energy E_F, the inelastic relaxation time τ, the temperature *T*, and the relaxation time $\tau = \mu E_{F/} ev_F^2$, expressed in turn in terms of the graphene Fermi velocity $v_F = c/300$ and the carrier mobility μ. We set the width of the graphene ribbon to 65 nm and a gap of 100 nm, following experimental data.

Using COMSOL Multiphysics simulation, we can calculate the extinction of graphene ribbons/mica heterostructure, as depicted in Supplementary Figure 8b.

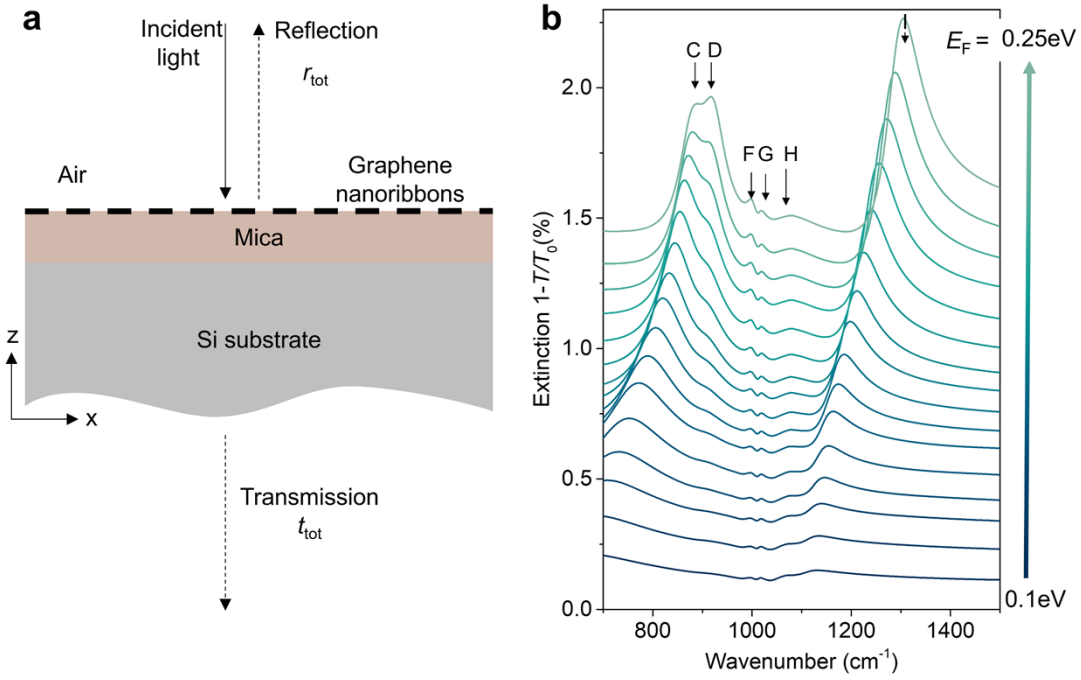

Supplementary Figure 8. Simulation of extinction spectra of graphene ribbons/mica-nanofilm heterostructure. (a) Schematic diagram illustrating the sample structure in the simulation. **(b)** Simulation extinction spectra of graphene nanoribbons under different Fermi energies E_F.

We would like to emphasize the discrepancy between our theoretical calculations and the experimental results. This discrepancy can be attributed to the highly complex phonon modes of mica, which become even more intricate when coupled with graphene plasmons. In the simulation data, certain peaks are missing, which occurs because the longitudinal phonons of mica, which are perpendicular to the far-field direction, are challenging to directly detect in the far field (Supplementary Figure 7b). Graphene plasmonic fields do not necessarily align with the wave vector direction, allowing them to respond to

these longitudinal dipoles and manifest in the extinction spectra (Figure 2 in the main text). Nevertheless, these phonons have not yet been accounted for in the above fitting, leading to the absence of some vibrational signals. Graphene plasmons can couple with various phonon modes, leading to complex peaks in the Fourier transform infrared (FTIR) spectrum. In our experiments, we have not yet been able to fully resolve the phonon modes of mica.